MDPI

Communication

Structural Characterization of 4-(4-Nitrophenyl)thiomorpholine, a Precursor in Medicinal Chemistry

Paul R. Palme [1], Richard Goddard [2], Peter Imming [1] and Rüdiger W. Seidel [1,*]

[1] Institut für Pharmazie, Martin-Luther-Universität Halle-Wittenberg, Wolfgang-Langenbeck-Straße 4, 06120 Halle (Saale), Germany; paul.palme@pharmazie.uni-halle.de (P.R.P.); peter.imming@pharmazie.uni-halle.de (P.I.)

[2] Max-Planck-Institut für Kohlenforschung, Kaiser-Wilhelm-Platz 1, 45470 Mülheim an der Ruhr, Germany; goddard@mpi-muelheim.mpg.de

[*] Correspondence: ruediger.seidel@pharmazie.uni-halle.de; Tel.: +49-345-55-25154

Abstract: 4-(4-nitrophenyl)thiomorpholine, the title compound, has been used as a precursor for the corresponding 4-thiomorpholinoaniline, which is a useful building block in medicinal chemistry. The crystal and molecular structures of the title compound, however, have not been described thus far. We synthesized the title compound by means of a nucleophilic aromatic substitution reaction of 4-fluoronitrobenzene and thiomorpholine and structurally characterized it by X-ray crystallography, DFT calculations, and Hirshfeld surface analysis. In the crystal, the molecule exhibits an approximately C_S-symmetric structure, with the nitrogen-bound 4-nitrophenyl group in a quasi axial position on the six-membered thiomorpholine ring in a low-energy chair conformation. The solid-state structure of the title compound is markedly different from that of its morpholine analogue. This can be ascribed to the formation of centrosymmetric dimers through intermolecular C–H⋯O weak hydrogen bonds involving the methylene groups adjacent to the sulfur atom and face-to-face aromatic stacking.

Keywords: thiomorpholine; nucleophilic aromatic substitution; crystal structure; Hirshfeld surface analysis; DFT calculation; hydrogen bonding

check for **updates**

1. Introduction

The title compound 4-(4-nitrophenyl)thiomorpholine (**1**) has been widely used as a precursor in medicinal chemistry, for example, in the fields of antidiabetic [1] and antimigraine drugs [2], kinase inhibitors [3–5], reverse transcriptase inhibitors [6], and antibiotic [7], antifungal [8–10], and antimycobacterial agents [11]. After the reduction of the nitro group in **1**, the resulting 4-thiomorpholinoaniline can be used as a building block in amide-coupling reactions. In drug development, the thiomorpholine group serves as a replacement of the morpholine group, with the sulfur atom increasing the lipophilicity and representing a metabolically soft spot due to easy oxidation. The latter property has also been used to prepare the corresponding sulfoxides and sulfones [6]. Compound **1** has attracted our interest as a precursor in the course of our studies on antimycobacterial squaramides [12]. To the best of our knowledge and based on a search of the Cambridge Structural Database (CSD) [13] via WebCSD in February of 2024, a crystal structure of **1** has not been published thus far. In this contribution, we report the structural characterization of **1** by X-ray crystallography, augmented by Hirshfeld surface analysis and DFT calculations on the free molecule.

2. Results and Discussion

2.1. Synthesis

We readily obtained compound **1** in a good yield in a nucleophilic substitution reaction of 4-fluoronitrobenzene and thiomorpholine by heating them in acetonitrile in the presence

of a base (Scheme 1). The product was identified by ^{1}H and ^{13}C NMR spectroscopy (Figures S1 and S2). Similar methods for the synthesis of **1** from 4-fluoronitrobenzene and thiomorpholine using different solvents and conditions have been disclosed in the patent literature [2,6]. The reaction also proved to be suitable for combinatorial synthesis of **1** and its derivatives [14]. In analogy, compound **1** could also be synthesized by the heating of 4-chloronitrobenzene and thiomorpholine in 1-butanol [8–10,15]. More recently, the preparation of **1** by a transition metal-free *N*-arylation of thiomorpholine with (4-nitrophenyl)(phenyl)iodonium triflate has been demonstrated [16].
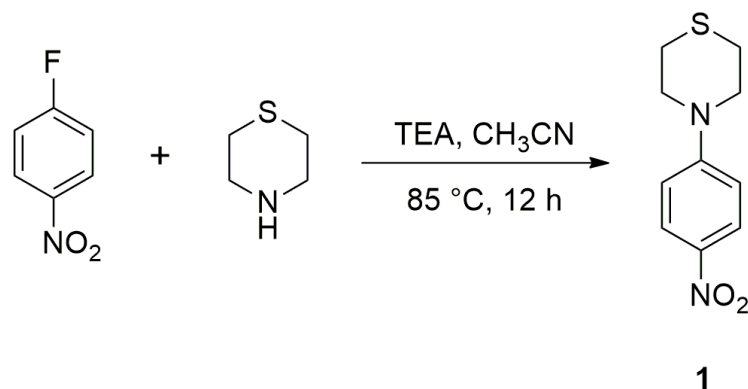
Scheme 1. Synthesis of **1** from 4-fluoronitrobenzene and thiomorpholine (TEA: triethylamine).

2.2. Solid-State Structure

Plate-shaped dark-yellow crystals of **1** were obtained from a solution in chloroform-*d*. The melting point of 142 °C agrees with that reported for **1** from ethanol in the literature (140–142 °C) [15]. Figure 1 shows the molecular structure of **1** in the crystal, as determined by X-ray crystallography. Table 1 lists selected geometric parameters. As expected, the thiomorpholine ring adopts a low-energy chair conformation. The C2–S1–C6 bond angle is smaller by ca. 10° than the regular tetrahedral angle of 109.5°. The 4-nitrophenyl group attached to N4 resides in a quasi axial position of the saturated six-membered ring. The molecular structure exhibits virtual C_S point group symmetry with an r.m.s. deviation of 0.06 Å. Interestingly, the morpholino analogue of **1** likewise shows a nearly C_S-symmetric structure in the crystal but with the 4-nitrophenyl group occupying a quasi equatorial position on the morpholine ring [17–19]. The structure overlay plot shown in Figure 1b illustrates the difference. The crystal structure of **1** features centrosymmetric dimers of the molecules through C–H···O weak hydrogen bonds [20] between the methylene groups adjacent to the sulfur and the two nitro oxygen atoms of the symmetry-related molecule (Table 2), resulting in an $R_2^2(8)$ motif [21], as well as face-to-face aromatic stacking (Figure 1c). The mean planes of the benzene rings are separated by 3.29 Å and the corresponding ring centroids by 4.26 Å. In the crystal, the dimers form close-packed layers with six-point coordination (Figure 2). The crystal packing is dense, as revealed by a calculated packing index of 74.4% [22].

To gain insight into the preferred conformation of the free molecule of **1**, we performed DFT calculations. Figure 1d shows the optimized molecular structure superimposed with the molecular structure in the crystal, and Table 1 compares selected geometric parameters. The 4-nitrophenyl group occupies a quasi equatorial position in the DFT-calculated structure rather than its quasi axial position in the crystal. Moreover, it is tilted with respect to the thiomorpholine ring, breaking the approximate molecular C_S symmetry encountered in the crystal (see the C–C–N–C torsion angles listed in Table 1). This suggests that the intermolecular interactions in the solid state have a bearing on the molecular conformation of **1**.
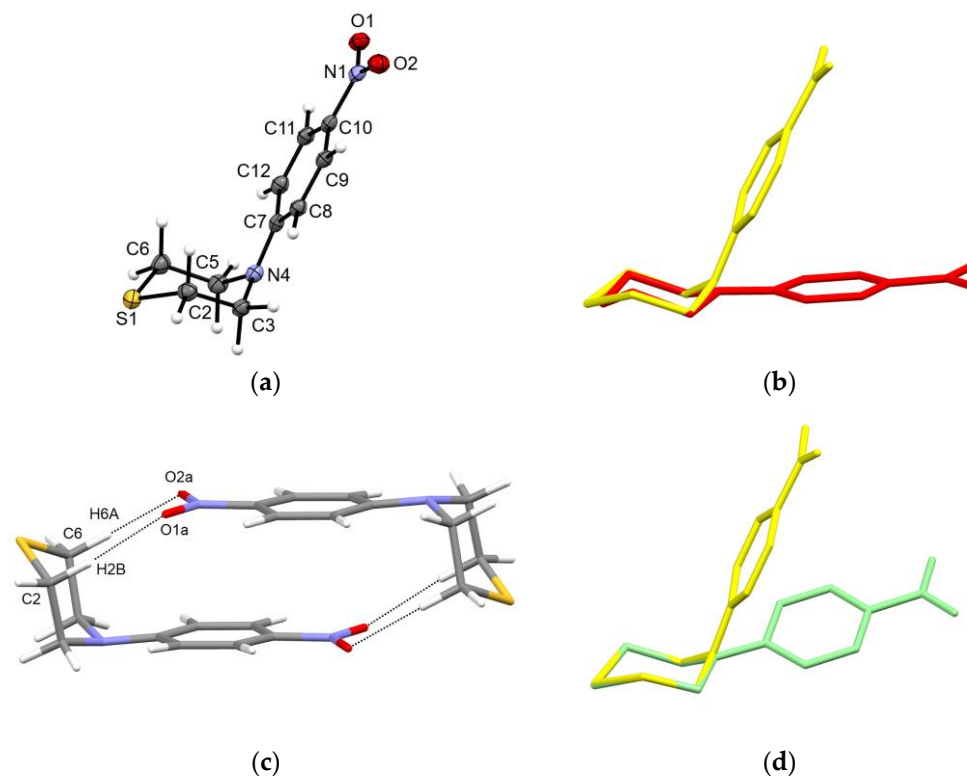
(a)

(b)

(c)

(d)

Figure 1. (**a**) Displacement ellipsoid plot (50% probability level) of **1**. Hydrogen atoms are shown by small spheres of arbitrary radii. (**b**) Structure overlay plot of **1** (yellow) and its morpholine analogue (red, CSD ref. code: YAYCIM01 [17]). (**c**) Centrosymmetric dimer of **1** in the crystal. Dashed lines represent C–H···O weak hydrogen bonds. (**d**) Structure overlay plot of **1** in the crystal (yellow) and the DFT-optimized structure (green). The structures in (**b**,**d**) are each overlaid at the respective methylene carbon atoms of the saturated rings. Hydrogen atoms are omitted for clarity in (**b**,**d**).

Table 1. Selected bond lengths, angles, and torsion angles for **1** (Å, °).

	X-ray	DFT
C2–C3	1.5249(18)	1.527
C2–S1	1.8193(13)	1.818
C3–N4	1.4681(16)	1.459
C5–C6	1.5271(18)	1.523
C5–N4	1.4632(16)	1.466
C6–S1	1.8178(15)	1.819
C7–N4	1.3804(15)	1.390
S1–C2–C3	111.06(9)	113.53
N4–C3–C2	111.58(10)	111.93
N4–C5–C6	111.24(11)	112.93
S1–C6–C5	111.60(9)	111.96
C5–N4–C3	111.49(10)	114.28
C6–S1–C2	99.56(6)	96.49
C3–N4–C7–C8	14.86(12)	10.93
C5–N4–C7–C12	−21.08(13)	41.71

Table 2. Selected hydrogen bond parameters for **1** (Å, °) [1].

D–H···*A*	*d*(*D*–H)	*d*(H–*A*)	*d*(*D*···*A*)	<(*DHA*)
C2–H2B···O1a	1.100(16)	2.313(16)	3.4086(15)	173.4(12)
C6–H6A···O2a	1.072(18)	2.498(18)	3.5126(16)	157.5(14)
C8–H8···O1b	1.075(15)	2.249(15)	3.3023(15)	165.9(12)

[1] Symmetry codes: (a) −x + 1, −y + 1, −z + 1; and (b) −x + 1, y − 1/2, −z + 1/2.
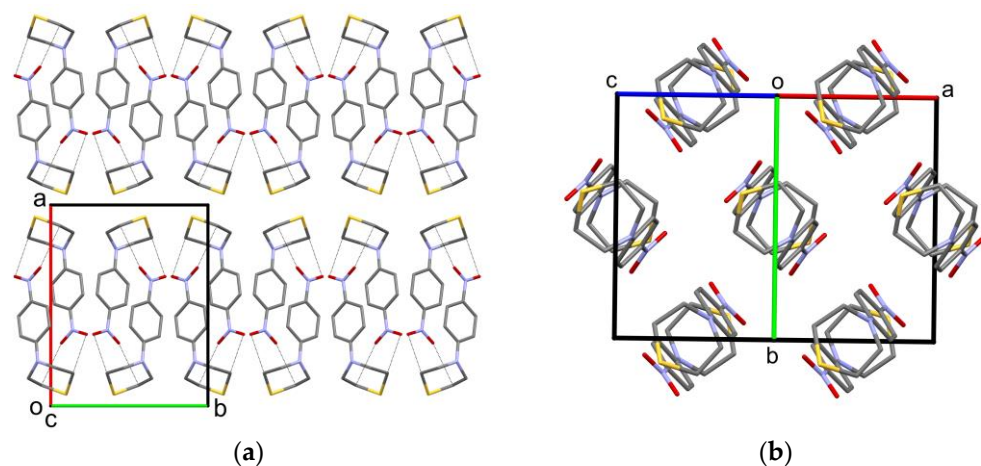
(**a**)　　　　　　　　　　(**b**)

Figure 2. Crystal structure of **1**, viewed (**a**) along the crystallographic *c*-axis direction, showing the sheet structure of the close-packed dimers, and (**b**) along the [101] direction, illustrating the close packing of the dimers within the sheets. Color scheme: C, grey; N, blue; O, red; and S, yellow. Hydrogen atoms are omitted for clarity.

To evaluate the crystal packing environment of the molecules in the crystal structure of **1** as a whole, we generated and visualized the Hirshfeld surface, mapped with the normalized contact distance (d_{norm}), as shown in Figure 3a [23]. The two C–H⋯O weak hydrogen bonds discussed in the previous paragraph show up as red areas (indicating contacts shorter than the van der Waals distance). An additional lateral red area on the Hirshfeld surface reveals a still shorter intermolecular C–H⋯O contact between the C8–H8 moiety of the phenyl ring and a nitro group oxygen atom (Table 2). The associated Hirshfeld surface fingerprint plot of the contact distance between the closest atom outside the surface (d_e) versus that of the nearest atom inside the surface (d_i), as depicted in Figure 3b, shows that, aside from the O⋯H contacts discussed above, S⋯H, C⋯H, and H⋯H contacts dominate the crystal structure. A feature characteristic of the C⋯C contacts from π⋯π stacking is not pronounced in the fingerprint plot. Contacts indicative of chalcogen bonding are not encountered.
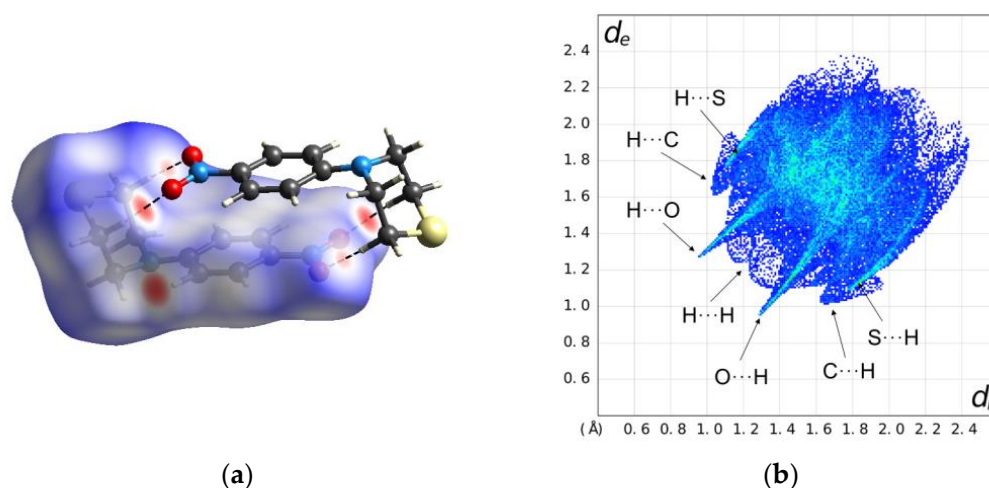

(**a**)　　　　　　　　　　(**b**)

Figure 3. (**a**) Hirshfeld surface plot for **1** mapped with d_{norm} (red areas indicate short contacts). Dashes lines represent C–H⋯O weak hydrogen bonds. Color scheme for the atoms: C, grey; H, white; N, blue; O, red; and S, yellow. (**b**) Hirshfeld surface fingerprint plot d_e versus d_i for **1**.

3. Materials and Methods

3.1. General

All chemicals were of reagent-grade quality and used as received. Solvents were distilled before use. The NMR spectra were recorded on an Agilent Technologies 400 MHz VNMRS spectrometer and evaluated using MestReNova (Mestrelab Research S.L., Santiago de Compostela, Spain). Chemical shifts are reported relative to the residual solvent peak of chloroform-*d* (δ_H = 7.24 ppm; δ_C = 77.05 ppm) as the internal standard. The HRMS analysis was performed on a Thermo Scientific™ Q Exactive™ GC Orbitrap™ GC-MS/MS instrument. The sample was dissolved in methanol. The melting point was determined on a Reichert Thermovar® hot stage and is reported uncorrected.

3.2. Synthesis

Thiomorpholine (1 mL, 10 mmol) and triethylamine (7 mL, 50 mmol) were placed in a 50 mL flask equipped with a reflux condenser, and 4-fluoronitrobenzene (10 mmol) dissolved in 15 mL of acetonitrile was added. The reaction mixture was stirred and heated to 85 °C for 12 h. After cooling to room temperature, 50 mL of deionized water were added, and the mixture was extracted with ethyl acetate (3 × 60 mL). The combined organic phases were dried over anhydrous sodium sulfate, and the solvent was removed under reduced pressure to yield 2.14 g (9.5 mmol, 95%) of **1**. ^{1}H NMR (402 MHz, chloroform-*d*) δ 8.08 (m, 2H), 6.75 (m, 2H), 3.82 (m, 4H), 2.68 (m, 4H) ppm. ^{13}C NMR (101 MHz, chloroform-*d*) δ 153.5, 138.1, 126.2, 112.8, 50.3, 25.8 ppm. HRMS (EI$^+$): m/z 224.061650, calculated for $[C_{10}H_{12}N_2O_2S]^+$ 224.061400.

3.3. X-ray Crystallography

Crystals of **1** suitable for a single-crystal X-ray diffraction analysis grew from a solution in chloroform-*d* in a standard NMR tube when the solvent evaporated slowly at ambient conditions. The crystals were coated with perfluoropolyether PFO-XR75 and mounted using a MiTeGen cryo-loop. The X-ray diffraction data were collected on a Bruker AXS D8 Venture diffractometer, equipped with an Incoatec IμS Diamond microfocus X-ray source, Incoatec multilayer optics, and a CMOS Photon III detector. The APEX4 software was used to operate the diffractometer and evaluate the diffraction data [24]. The data were processed with the SAINT software [25] and corrected for absorption effects with SADABS-2016/2 [26], using the Gaussian method based on indexed crystal faces.

The crystal structure was solved with SHELXT [27], and an initial independent atom model (IAM) refinement was carried out with SHELXL-2019/3 [28]. The structure was subsequently refined using NoSpherA2 [29,30] in Olex2 [31,32], with the Hirshfeld partioning of the electron density calculated using ORCA 5.0 [33] (B3LYP [34,35]/de2-TZVPP [36]). Anisotropic atomic displacement parameters were introduced for non-hydrogen atoms. The structure pictures were generated with Mercury [37]. The packing index was calculated with Platon [38]. The Hirshfeld surface analysis was conducted with CrystalExplorer [39].

Crystal data and refinement details for **1**: $C_{10}H_{12}N_2O_2S$, M_r = 224.285, T = 100(2) K, λ = 0.71073 Å, monoclinic, space group $P2_1/c$, a = 13.3525(5), b = 10.3755(4), c = 7.4464(3) Å, β = 96.325(2)°, V = 1025.34(7) Å^3, Z = 4, ρ_{calc} = 1.453 g cm^{-3}, μ_{calc} = 0.296 mm^{-1}, $F(000)$ = 472.78, crystal size = 0.153 × 0.055 × 0.031 mm, θ range = 2.49–30.53°, 114,201 reflections collected, 3136 reflections unique, R_{int} = 0.0839, observed reflections [$I > 2\sigma(I)$] 2478, 0 restraints, 184 parameters, $R1$ [$I > 2\sigma(I)$] = 0.0324, $wR2$ (all data) = 0.0811, $\Delta\rho_{max}$ = 0.3886 eÅ^{-3}, and $\Delta\rho_{min}$ = −0.4092 eÅ^{-3}.

3.4. Computational Methods

DFT calculations were performed using ORCA 5.0 [33] with a B3LYP/G (VWN5) hybrid functional (20% HF exchange) [34,36,40], using a def2-TZVPP basis set [36] with an auxiliary def2/J basis [41]. The optimization of the structure used the BFGS method from an initial Hessian according to Almlöf's model, with a very tight self-consistent field convergence threshold [42]. The calculations were made on the free molecule of **1**. The optimized

local minimum-energy structure exhibited only positive modes. The Cartesian coordinates of the DFT-optimized structure of **1** can be found in the Supplementary Materials. The structure pictures were generated with Mercury [37].

4. Conclusions

We have determined the crystal and molecular structure of **1** by X-ray crystallography. In contrast to the previously known structure, the morpholino analogue, the approximately C_S-symmetric molecules of **1** exhibit a bent conformation in the crystal and pack centrosymmetrically as dimers through C–H···O weak hydrogen bonds between the methylene groups attached to the sulfur and the oxygen atoms of a nitro group in an adjacent molecule. The DFT calculations of the energy-minimized structure of the isolated molecule indicate that intermolecular interactions and packing effects affect the conformation of **1** in the solid state. The capacity of the 4-phenylthiomorpholine group to participate in weak interactions such as C–H···O hydrogen bonds revealed in the crystal structure of **1** may have implications for target binding.

References

1. Schwink, L.; Stengelin, S.; Gossel, M. *WO2003015769*; Preparation of Indol-5-ylureas and Relate Compounds for the Treatment of Obesity and Type II Diabetes. 2003.
2. Chapdelaine, M.; Davenport, T.; Haeberlein, M.; Horchler, C.; McCauley, J.; Pierson, E.; Sohn, D. *WO2002055014*; Preparation of Piperazinylchromans as 5-HT1B and 5-HT1D Agonists/Antagonists Useful as Antimigraine Drugs. 2002.
3. Li, Y.; Ye, T.; Xu, L.; Dong, Y.; Luo, Y.; Wang, C.; Han, Y.; Chen, K.; Qin, M.; Liu, Y.; et al. Discovery of 4-piperazinyl-2-aminopyrimidine derivatives as dual inhibitors of JAK2 and FLT3. *Eur. J. Med. Chem.* **2019**, *181*, 111590. [CrossRef] [PubMed]
4. Hu, G.; Wang, C.; Xin, X.; Li, S.; Li, Z.; Zhao, Y.; Gong, P. Design, synthesis and biological evaluation of novel 2,4-diaminopyrimidine derivatives as potent antitumor agents. *New J. Chem.* **2019**, *43*, 10190–10202. [CrossRef]
5. Hou, Y.; Zhu, L.; Li, Z.; Shen, Q.; Xu, Q.; Li, W.; Liu, Y.; Gong, P. Design, synthesis and biological evaluation of novel 7-amino-[1,2,4]triazolo[4,3-f]pteridinone, and 7-aminotetrazolo[1,5-f]pteridinone derivative as potent antitumor agents. *Eur. J. Med. Chem.* **2019**, *163*, 690–709. [CrossRef] [PubMed]
6. Andrews, C.W.; Chan, J.H.; Freeman, G.A.; Romines, K.R.; Tidwell, J.H. *Preparation of benzophenones and phenyl heteroaryl ketones as inhibitors of reverse transcriptase* **2001**.
7. Gordeev, M.F.; Renslo, A.; Luehr, G.W.; Lam, S.; Westlund, N.E.; Patel, D.V. *Preparation of Antibacterial Dihydrothiazinyl and Dihydrothiopyranyl Oxazolidinones* **2003**.
8. Thomson, S.P.; Davies, R.T.; Allanson, N.M.; Kuvshinov, A.; Davies, G.M.; Edwards, P.N. *WO2006123145*; Preparation of Indolizinyloxoacetamides and Related Compounds as Medical and Agrochemical Fungicides. 2006.

9. Downham, R.; Sibley, G.E.M.; Payne, L.J.; Edwards, P.; Davies, G.M. *WO2008062182*; 2-[(2-Substituted)-Indolizolin-3-yl]-2-Oxoacetamide Derivatives as Antifungal Agents and Their Preparation, Pharmaceutical and Agricultural Compositions and Use in the Treatment of Fungal Diseases. 2008.

10. Birch, M.; Sibley, G.E.M.; Law, D.; Oliver, J.D. *WO2009144473*; Preparation of Indolizine Compounds for Use in Antifungal Combination Therapy. 2009.

11. Mai, A.; Sbardella, G.; Artico, M.; Massa, S.; Lampis, G.; Deidda, D.; Pompei, R. N-[4-(1,1′-biphenylyl)methyl]-4-(4-thiomorpholinylmethyl) benzenamines, a new class of synthetic antituberculosis agents active against Mycobacterium avium. *Med. Chem. Res.* **1999**, *9*, 149–161.

12. Courbon, G.M.; Palme, P.R.; Mann, L.; Richter, A.; Imming, P.; Rubinstein, J.L. Mechanism of mycobacterial ATP synthase inhibition by squaramides and second generation diarylquinolines. *EMBO J.* **2023**, *42*, e113687. [CrossRef] [PubMed]

13. Groom, C.R.; Bruno, I.J.; Lightfoot, M.P.; Ward, S.C. The Cambridge Structural Database. *Acta Crystallogr. B* **2016**, *72*, 171–179. [CrossRef]

14. Trump, R.P.; Blanc, J.-B.E.; Stewart, E.L.; Brown, P.J.; Caivano, M.; Gray, D.W.; Hoekstra, W.J.; Willson, T.M.; Han, B.; Turnbull, P. Design and Synthesis of an Array of Selective Androgen Receptor Modulators. *J. Comb. Chem.* **2007**, *9*, 107–114. [CrossRef]

15. Beach, S.F.; Hepworth, J.D.; Sawyer, J.; Hallas, G.; Marsden, R.; Mitchell, M.M.; Ibbitson, D.A.; Jones, A.M.; Neal, G.T. Dipole moments of some N-phenyl-substituted derivatives of pyrrolidine, piperidine, morpholine, and thiomorpholine. *J. Chem.Soc. Perkin Trans. 2* **1984**, 217–221. [CrossRef]

16. Purkait, N.; Kervefors, G.; Linde, E.; Olofsson, B. Regiospecific N-Arylation of Aliphatic Amines under Mild and Metal-Free Reaction Conditions. *Angew. Chem. Int. Ed. Engl.* **2018**, *57*, 11427–11431. [CrossRef]

17. White, J.M.; Fellows, T. CSD Communication 2016. [CrossRef]

18. White, J.M.; Skene, C.E.; Deadman, J.; Epa, R.; Foenander, S.; Hamer, K.; Fellowes, T.; Lim, S.F.; Marcuccio, S.M.; Martin, R.F. Synthesis and Structural Investigation of Some Electron-Rich Nitroaromatics. *Aust. J. Chem.* **2019**, *72*, 311–327. [CrossRef]

19. Wang, L.J.; Li, W.W.; Yang, S.Y.; Yang, L. 4-(4-Nitro-phen-yl)morpholine. *Acta Crystallogr. E* **2012**, *68*, o1235. [CrossRef]

20. Thakuria, R.; Sarma, B.; Nangia, A. 7.03-Hydrogen Bonding in Molecular Crystals. In *Comprehensive Supramolecular Chemistry II*; Atwood, J.L., Ed.; Elsevier: Oxford, UK, 2017; pp. 25–48.

21. Bernstein, J.; Davis, R.E.; Shimoni, L.; Chang, N.L. Patterns in Hydrogen Bonding: Functionality and Graph Set Analysis in Crystals. *Angew. Chem. Int. Ed.* **1995**, *34*, 1555–1573. [CrossRef]

22. Kitajgorodskij, A.I. *Molecular Crystals and Molecules*; Academic Press: New York, NY, USA, 1973.

23. Spackman, M.A.; Jayatilaka, D. Hirshfeld surface analysis. *CrystEngComm* **2009**, *11*, 19–32. [CrossRef]

24. Bruker. *APEX4*; Bruker AXS Inc.: Madison, WI, USA, 2017.

25. Bruker. *SAINT V8.40B*; Bruker AXS Inc.: Madison, WI, USA, 2019.

26. Bruker. *SADABS*; Bruker AXS Inc.: Madison, WI, USA, 2012.

27. Sheldrick, G.M. SHELXT-integrated space-group and crystal-structure determination. *Acta Crystallogr. A* **2015**, *71*, 3–8. [CrossRef] [PubMed]

28. Sheldrick, G.M. Crystal structure refinement with SHELXL. *Acta Crystallogr. C* **2015**, *71*, 3–8. [CrossRef] [PubMed]

29. Kleemiss, F.; Dolomanov, O.V.; Bodensteiner, M.; Peyerimhoff, N.; Midgley, L.; Bourhis, L.J.; Genoni, A.; Malaspina, L.A.; Jayatilaka, D.; Spencer, J.L.; et al. Accurate crystal structures and chemical properties from NoSpherA2. *Chem. Sci.* **2021**, *12*, 1675–1692. [CrossRef]

30. Midgley, L.; Bourhis, L.J.; Dolomanov, O.V.; Grabowsky, S.; Kleemiss, F.; Puschmann, H.; Peyerimhoff, N. Vanishing of the atomic form factor derivatives in non-spherical structural refinement—A key approximation scrutinized in the case of Hirshfeld atom refinement. *Acta Crystallogr. A* **2021**, *77*, 519–533. [CrossRef]

31. Dolomanov, O.V.; Bourhis, L.J.; Gildea, R.J.; Howard, J.A.K.; Puschmann, H. OLEX2: A complete structure solution, refinement and analysis program. *J. Appl. Crystallogr.* **2009**, *42*, 339–341. [CrossRef]

32. Bourhis, L.J.; Dolomanov, O.V.; Gildea, R.J.; Howard, J.A.K.; Puschmann, H. The anatomy of a comprehensive constrained, restrained refinement program for the modern computing environment-Olex2 dissected. *Acta Crystallogr. A* **2015**, *71*, 59–75. [CrossRef]

33. Neese, F.; Wennmohs, F.; Becker, U.; Riplinger, C. The ORCA quantum chemistry program package. *J. Chem. Phys.* **2020**, *152*, 224108. [CrossRef] [PubMed]

34. Becke, A.D. Density-functional thermochemistry. III. The role of exact exchange. *J. Chem. Phys.* **1993**, *98*, 5648–5652. [CrossRef]

35. Lee, C.; Yang, W.; Parr, R.G. Development of the Colle-Salvetti correlation-energy formula into a functional of the electron density. *Phys. Rev. B* **1988**, *37*, 785–789. [CrossRef]

36. Weigend, F.; Ahlrichs, R. Balanced basis sets of split valence, triple zeta valence and quadruple zeta valence quality for H to Rn: Design and assessment of accuracy. *Phys. Chem. Chem. Phys.* **2005**, *7*, 3297–3305. [CrossRef]

37. Macrae, C.F.; Sovago, I.; Cottrell, S.J.; Galek, P.T.A.; McCabe, P.; Pidcock, E.; Platings, M.; Shields, G.P.; Stevens, J.S.; Towler, M.; et al. Mercury 4.0: From visualization to analysis, design and prediction. *J. Appl. Crystallogr.* **2020**, *53*, 226–235. [CrossRef]

38. Spek, A.L. Structure validation in chemical crystallography. *Acta Crystallogr. D* **2009**, *65*, 148–155. [CrossRef] [PubMed]

39. Spackman, P.R.; Turner, M.J.; McKinnon, J.J.; Wolff, S.K.; Grimwood, D.J.; Jayatilaka, D.; Spackman, M.A. CrystalExplorer: A program for Hirshfeld surface analysis, visualization and quantitative analysis of molecular crystals. *J. Appl. Crystallogr.* **2021**, *54*, 1006–1011. [CrossRef] [PubMed]

40.   Hertwig, R.H.; Koch, W. On the parameterization of the local correlation functional. What is Becke-3-LYP? *Chem. Phys. Lett.* **1997**, *268*, 345–351. [CrossRef]
41.   Weigend, F. Accurate Coulomb-fitting basis sets for H to Rn. *Phys. Chem. Chem. Phys.* **2006**, *8*, 1057–1065. [CrossRef]
42.   Fletcher, R. *Practical Methods of Optimization*, 2nd ed.; John Wiley & Sons: Hoboken, NJ, USA, 2000.